

Scalable and Communication-Efficient Varying Coefficient Mixed Effect Models: Methodology, Theory, and Applications

Lida Chalangar Jalili Dehkharghani¹ and Li-Hsiang Lin¹

¹Department of Mathematics and Statistics,
Georgia State University, Atlanta, GA, 30303

November 18, 2025

Abstract

Human migration exhibits complex spatiotemporal dependence driven by environmental and socioeconomic forces. Modeling such patterns at scale—often across multiple administrative or institutional boundaries—requires statistically efficient methods that remain robust under limited communication, i.e., when transmitting raw data or large design matrices across distributed nodes is costly or restricted. This paper develops a communication-efficient inference framework for Varying Coefficient Mixed Models (VCMMs) that accommodates many input variables in the mean structure and rich correlation induced by numerous random effects in hierarchical migration data. We show that a penalized spline estimator admit a Bayesian hierarchical representation, which in turn yields sufficient statistics that preserve the full likelihood contribution of each node when communication is unconstrained; aggregating these summaries reproduces the centralized estimator exactly. Under communication constraints, the same summaries define a surrogate likelihood enabling one-step estimation with first-order statistical efficiency. The framework also incorporates an SVD-enhanced implementation to ensure numerical stability and scalability, extending applicability to settings with many random effects, with or without communication limits. Statistical and theoretical guarantees are provided. Extensive simulations confirm the accuracy and robustness of the method. An application to U.S. migration flow data demonstrates its ability to efficiently and precisely uncover dynamic spatial patterns.

Keywords: Big Data Computation, Varying Coefficient Models, Sufficient Statistics, SVD Decomposition, Random Effects, Distributed Computing

1 Introduction

Human migration reflects the complex interplay of environmental, socioeconomic, and policy forces, exhibiting rich spatial–temporal dependencies. Accelerating climate change has intensified environmental stressors, driving large-scale displacements and raising pressing questions about urban resilience and resource allocation (McMichael et al., 2012). For instance, recurrent hurricanes and flooding in coastal Louisiana have triggered sustained population outflows, reshaping communities and straining infrastructure (Paglino, 2024). The increasing availability of large-scale migration records offers unprecedented opportunities for quantitative analysis. These datasets—often containing millions of observations with hierarchical, correlated, and spatially structured components—pose formidable computational and inferential challenges. Moreover, administrative boundaries and data-governance policies often restrict the amount of data exchange across institutions—or even among computing nodes within high-performance systems—making centralized data pooling infeasible due to the prohibitive cost of transferring large matrices. These challenges motivate the need for statistical frameworks that are simultaneously scalable, communication-efficient, and capable of achieving statistical optimality under the communication constraints.

These unique characteristics—large scale, hierarchical dependence, spatial structure, and strict communication constraints—substantially limit the applicability of classical regression-based approaches for migration modeling. A central object of interest is the *Origin–Destination (OD) flow*, which records the number of individuals relocating between two regions over time (Fields, 1979; Gurak and Caces, 1992). Because OD flows are shaped by evolving covariates such as climate indices and economic indicators, flexible varying-coefficient models (Hastie and Tibshirani, 1993; Hoover et al., 1998; Moore et al., 2020) provide a natural modeling strategy. These models allow regression effects to evolve smoothly over time, space, or other contextual variables (Lu and Zhang, 2009; Cai et al., 2021; Chen et al., 2025), making them well suited for capturing dynamic migration mechanisms. At the same time, flows between origins and destinations exhibit strong correlations induced by shared environmental

conditions, regional structures, and unobserved local factors. Such dependencies motivate random-effect formulations (Wang and Huang, 2008; Li and Wang, 2010; Chen and Wang, 2011; Morris and Carroll, 2006), which effectively capture heterogeneous covariate responses across origins, destinations, and time. Moreover, these two modeling components—smoothly varying coefficients and hierarchical random effects—have also been considered jointly within unified regression frameworks (Tutz and Kauermann, 2003; Zhang and Shen, 2015; Li et al., 2020; Hung et al., 2022), which we refer to as Varying Coefficient Mixed Models (VCMMs). However, existing VCMM methodologies are typically designed for settings with a modest number of random effects and assume centralized computation without communication constraints. They do not scale to modern migration datasets that involve many thousands of OD pairs, high-dimensional random effects, and distributed data storage. Consequently, there is a pressing need for a new modeling and computational framework that simultaneously (i) captures smooth coefficient trajectories and high-dimensional hierarchical random effects, and (ii) enables reliable estimation under strict communication and memory constraints.

To address this challenge, we establish a fundamental equivalence between VCMM estimation based on spline expansion (Wahba, 1978; Silverman, 1985; Eilers and Marx, 1996; Ruppert et al., 2003; Wood, 2017) and a Bayesian hierarchical formulation. Specifically, the penalized spline estimators of varying coefficients with random effects correspond exactly to the posterior means under an appropriately constructed hierarchical model. To the best of our knowledge, while prior studies have explored connections between Bayesian frameworks and varying-coefficient regression with penalized estimation (Franco-Villoria et al., 2019; Chen et al., 2025), extensions that incorporate random effects, large-scale data, or communication constraints remain largely unexplored. Our connection provides a principled likelihood interpretation of VCMMs and identifies a compact set of *sufficient statistics*—low-dimensional cross-products of design and response matrices—that fully characterize the posterior means. Crucially, these sufficient statistics can be computed independently across distributed data partitions or multiple nodes and then aggregated without loss of likelihood

information, enabling fully parallelizable and exact maximum likelihood estimation. When the number of random effects is large, our algorithm can be equipped with large-scale SVD (Halko et al., 2011; Liberty et al., 2007; Meng et al., 2014; Qiu et al., 2024) to stabilize inversion of the associated covariance operator from the random effects. Such an implementation is generally unnecessary in conventional mixed-effects models, where the random-effects structure is low-dimensional and/or block-diagonal (Lindstrom and Bates, 1988; Dunson et al., 2008), allowing sparse Cholesky factorization to suffice. This scalable spectral formulation provides robustness and efficiency in regimes where classical mixed-model solvers deteriorate.

When communication constraints become the dominant bottleneck, our sufficient-statistics framework extends naturally to approximate a surrogate likelihood that enables one-step estimation of both varying-coefficient and random-effect parameters without iterative data exchange. This framework can be further enhanced for larger-scale applications through suitable SVD-based decomposition techniques, as discussed earlier for the setting without communication constraints. In contrast, existing distributed estimation strategies—such as divide-and-conquer (Zhang et al., 2015; Chen and Xie, 2014), distributed kernel regression (Zhang et al., 2015), and communication-efficient sparse learning (Wang et al., 2017; Jordan et al., 2019; Lee et al., 2017; Fan et al., 2023)—achieve scalability for independent observations but fail to accommodate the spatial, longitudinal, or clustered dependence structures that are fundamental to migration analysis. Recent developments have begun to address distributed modeling for varying-coefficient structures (Huang and Huo, 2019; Guhaniyogi et al., 2022) or random effects (Luo et al., 2022), but not both simultaneously, and typically rely on iterative communication or restrictive modeling assumptions. Furthermore, our framework is supported by rigorous theoretical guarantees. The proposed estimator enjoys asymptotic efficiency, non-asymptotic concentration bounds, and communication optimality, demonstrating that statistical accuracy and efficiency can be preserved even under stringent communication limitations. Overall, our approach attains the same first-order statistical efficiency for estimating varying-coefficient and random-effect parameters as the conventional

centralized maximum likelihood estimator that would be obtained if all raw data were pooled without communication constraints.

Although motivated by migration studies, the proposed framework is broadly applicable since varying coefficients and random effects are widely used across diverse scientific domains. Consequently, our method can be extended to other areas characterized by large, structured, correlated, and distributed data, including spatiotemporal climate modeling, large-scale biomedical research, neuroimaging analysis, and sensor network inference. The ability to perform likelihood-based inference with minimal communication ensures both scalability and statistical optimality in these complex settings.

The remainder of the paper is organized as follows. Section 2 formulates the objective function of the varying-coefficient mixed-effects model under communication constraints and introduces the VCMM framework. Section 3 develops its matrix representation, the sufficient-statistics-based likelihood, and theoretical properties ensuring convergence and numerical stability. Section 4 presents the communication-efficient one-step estimation procedure, including the SVD-stabilized implementation based on aggregated sufficient statistics. This section also establishes the asymptotic efficiency and non-asymptotic finite-sample guarantees of the proposed estimator. Section 5 reports comprehensive numerical studies, and Section 6 illustrates the method through a large-scale migration analysis. Finally, Section 7 concludes with future research directions. The supplemental material collect technical proofs, algorithmic details, and additional numerical results.

2 Varying Coefficient Mixed Effects Models with Communication Constraint

The Varying Coefficient Mixed Model (VCMM) is designed to capture complex, structured dependencies in spatiotemporal and hierarchical data. Throughout this paper, we consider migration flow data observed across I origins and J destinations. Let y_{ijt} denote the migra-

tion response from origin i to destination j at time t , associated with covariates \mathbf{x}_{ijt} (fixed effects) and \mathbf{z}_{ijt} (random effects). The VCMM is specified as

$$y_{ijt} = \beta_0(\mathbf{h}_{ijt}) + \sum_{k=1}^p x_{k,ijt} \beta_k(\mathbf{h}_{ijt}) + \mathbf{z}_{ijt}^\top \boldsymbol{\alpha} + \epsilon_{ijt}, \quad (1)$$

where the index variable \mathbf{h}_{ijt} collects temporal, spatial, and socio-economic features that influence migration dynamics. Each coefficient function $\beta_k(\mathbf{h}_{ijt})$ varies smoothly with \mathbf{h}_{ijt} and is represented using tensor-product B-spline basis expansions. The random effects satisfy $\boldsymbol{\alpha} \sim N(\mathbf{0}, \boldsymbol{\Sigma}_\alpha)$ with $\dim(\boldsymbol{\alpha}) = q$, and the noises follow $\epsilon_{ijt} \sim N(0, \sigma_\epsilon^2)$. Given model (1), the likelihood of the observed data and random effects is expressed through their joint distribution,

$$\ell_{\text{joint}}(\boldsymbol{\beta}(\mathbf{h}), \boldsymbol{\alpha}, \boldsymbol{\eta}) \equiv p(\mathbf{y}, \boldsymbol{\alpha} \mid \boldsymbol{\beta}(\mathbf{h}), \boldsymbol{\eta}) = p(\mathbf{y} \mid \boldsymbol{\beta}(\mathbf{h}), \boldsymbol{\alpha}, \sigma_\epsilon^2) p(\boldsymbol{\alpha} \mid \boldsymbol{\Sigma}_\alpha), \quad (2)$$

where $\boldsymbol{\eta} = (\boldsymbol{\Sigma}_\alpha, \sigma_\epsilon^2)$ collects the variance components. This formulation simultaneously captures the hierarchical dependence induced by the random effects and the smooth variation of the coefficient functions with respect to the index variable \mathbf{h}_{ijt} .

In large-scale applications, data are often distributed across multiple computational nodes or data centers due to administrative restrictions or the practical burden of storing and processing massive datasets. Transmitting raw observations or high-dimensional spline design matrices between nodes is computationally prohibitive. To address this issue, each node performs local computations and communicates only compact sufficient summaries to a central server, thereby reducing communication burden while preserving all information necessary for likelihood-based inference. Accordingly, the distributed estimation problem can be written as

$$\max_{\boldsymbol{\beta}(\mathbf{h}), \boldsymbol{\alpha}, \boldsymbol{\eta}} \ell_{\text{joint}}(\boldsymbol{\beta}(\mathbf{h}), \boldsymbol{\alpha}, \boldsymbol{\eta}) \quad \text{subject to} \quad \text{total bits communicated} \leq cdk, \quad (3)$$

where d is the dimension of the parameter vector, k is the number of distributed nodes, and c

is a universal constant. This constraint captures the fundamental trade-off between statistical accuracy and communication efficiency: richer local summaries improve estimation precision but require more communication resources, with cdk representing the minimal information needed for minimax-optimal distributed inference.

The importance of the communication constraint in (3) becomes evident when considering how modeling choices directly influence the parameter dimension d and thus the total communication cost. For example, accurate approximation of the varying coefficients $\beta_k(\mathbf{h})$ requires sufficiently rich B-spline bases; however, enlarging the basis dimension increases the number of spline coefficients and causes the matrices transmitted from each node to grow quadratically. Too few basis functions lead to underfitting, while too many induce overfitting and impose prohibitive communication cost in a distributed environment. A similar trade-off arises in specifying the random-effect structure: modeling regional heterogeneity may require multiple random-effect components (e.g., origin, destination, or origin–destination interactions), but each additional component enlarges the dimension of $\boldsymbol{\alpha}$ and increases the size of the associated Gram matrices that must be communicated or aggregated. In centralized analysis, such modeling decisions are routinely handled using AIC, BIC, REML-based likelihood comparisons, or cross-validation—procedures that repeatedly refit the model across many candidate specifications. Under strict communication limits, however, repeated refitting is infeasible because each evaluation would exceed the allowable communication budget. Together, these examples illustrate the core difficulty posed by (3): high-quality inference requires balancing approximation fidelity with communication efficiency, motivating the development of methods that remain statistically robust under stringent constraints. Practical limitations—such as caps on data transfer, distributed storage architectures, and the organization of our motivating migration dataset—further reinforce the necessity of communication-aware estimation strategies.

Beyond these concrete examples, incorporating a communication budget into the problem formulation provides methodological advantages even in settings where communication

constraints are not explicitly binding. Framing the estimation problem under (3) offers a principled perspective for designing algorithms that remain computationally efficient, scalable, and robust across heterogeneous computing environments. It also clarifies the statistical implications of information flow in distributed systems: understanding how joint likelihood estimators behave under a communication limit highlights the fundamental trade-off between information exchange and estimation accuracy. Moreover, this formulation naturally structures the methodological development that follows. Section 3 examines the idealized regime with no communication constraint ($c = \infty$), establishing the statistical and computational foundations of the proposed estimation procedure. Section 4 then builds upon these results to address the realistic case $c < \infty$, where communication-efficient algorithms are required. Considering both regimes provides a unified framework for VCMM estimation in centralized and distributed settings and lays the groundwork for the developments in the subsequent sections.

3 Distributed and Scalable Estimation for Varying Coefficient Mixed Effects Models

To build the methodological foundation for communication-aware inference, we first analyze the idealized centralized regime with no communication constraint ($c = \infty$), where all data and design matrices can be jointly accessed. Studying this unconstrained setting is essential for two reasons. First, it establishes a statistical and computational benchmark against which distributed procedures can be evaluated. Second, the centralized formulation reveals the key algebraic structures—particularly the blockwise updates and sufficient-statistics representation—that enable scalable extensions of VCMMs to large-scale, distributed environments. The results developed in this section therefore serve as the baseline upon which the communication-constrained methods of Section 4 are built, ultimately allowing us to address high-dimensional covariates and complex random-effect structures under realistic

communication limitations.

3.1 A Bayesian Perspective under No Communication Cost: Posterior Characterization and Connection with Sufficient Statistics

Under no communication constraint ($c = \infty$ in (3)), all observations are available on a single node, enabling direct estimation of the model parameters through a unified Bayesian framework. We first reformulate the VCMM in matrix form using B-spline basis expansions, which provides the foundation for deriving the posterior distribution and its sufficient-statistics representation.

To construct the B-spline design, suppose Q knots are chosen for the basis expansion and M components are present in \mathbf{h}_{ijt} . Then each varying coefficient function admits the representation

$$\beta_k(\mathbf{h}_{ijt}) = \sum_{q=1}^Q \gamma_{kq} \Phi_q(\mathbf{h}_{ijt}), \quad (4)$$

where $\Phi_q(\mathbf{h}_{ijt}) = \prod_{m=1}^M \phi_q^{(m)}(h_{ijt}^{(m)})$ is a tensor-product basis constructed from univariate B-splines $\phi_q^{(m)}(\cdot)$ along each dimension m , efficiently implemented via the Cox–de Boor recursion formula (De Boor, 1978). Collecting all coefficients yields

$$\tilde{\boldsymbol{\beta}} = (\gamma_{01}, \dots, \gamma_{0Q}, \gamma_{11}, \dots, \gamma_{1Q}, \dots, \gamma_{p1}, \dots, \gamma_{pQ})^\top.$$

Applying (4) to (1) expands the original model matrix \mathbf{X} into a higher-dimensional tensor-product B-spline model matrix $\tilde{\mathbf{X}}$. Each original predictor $x_{k,ijt}$ is multiplied by the Q basis evaluations $\{\Phi_q(\mathbf{h}_{ijt})\}_{q=1}^Q$, yielding pQ basis-augmented columns (plus Q basis terms for the intercept). Consequently, the stacked model across all (i, j, t) observations becomes

$$\mathbf{y} = \tilde{\mathbf{X}} \tilde{\boldsymbol{\beta}} + \mathbf{Z} \boldsymbol{\alpha} + \boldsymbol{\epsilon}, \quad (5)$$

where \mathbf{y} is the stacked vector of all responses $\{y_{ijt}\}$ across origins, destinations, and time,

$\tilde{\mathbf{X}}$ encodes the tensor-product B-spline expansions of \mathbf{h}_{ijt} , $\tilde{\boldsymbol{\beta}}$ collects the corresponding basis coefficients, and \mathbf{Z} is the random-effect model matrix. Model (5) form the basis for the subsequent Bayesian and sufficient-statistics formulations, illustrating how the expanded design flexibly captures spatiotemporal heterogeneity in migration dynamics.

We first develop a Bayesian framework to ensure stable estimation and coherent uncertainty quantification. Assume the priors

$$\tilde{\boldsymbol{\beta}} \sim N(\mathbf{0}, \mathbf{P}_{\lambda^*}^{-1}), \quad \boldsymbol{\alpha} \sim N(\mathbf{0}, \boldsymbol{\Sigma}_{\alpha}), \quad \boldsymbol{\epsilon} \sim N(\mathbf{0}, \sigma_{\epsilon}^2 \mathbf{I}), \quad (6)$$

where \mathbf{P}_{λ^*} is a ridge-type penalty matrix controlling the smoothness of $\tilde{\boldsymbol{\beta}}$. Combining (5) and (6) yields the posterior distribution under the centralized setting, which later provides the foundation for communication-efficient sufficient-statistics aggregation.

Theorem 3.1 (Equivalence between an VCMM estimation and a Bayesian hierarchical model). *Under the VCMM and Gaussian prior assumptions in (6), the joint posterior of $(\tilde{\boldsymbol{\beta}}, \boldsymbol{\alpha})$ given \mathbf{y} is multivariate normal:*

$$\begin{pmatrix} \tilde{\boldsymbol{\beta}} \\ \boldsymbol{\alpha} \end{pmatrix} \left| \mathbf{y} \sim N(\boldsymbol{\mu}, \boldsymbol{\Sigma}), \right.$$

where

$$\boldsymbol{\mu} = \boldsymbol{\Sigma} \begin{pmatrix} \frac{1}{\sigma_{\epsilon}^2} \tilde{\mathbf{X}}^T \mathbf{y} \\ \frac{1}{\sigma_{\epsilon}^2} \mathbf{Z}^T \mathbf{y} \end{pmatrix}, \quad \boldsymbol{\Sigma}^{-1} = \begin{pmatrix} \mathbf{V}_{\beta} & \mathbf{V}_{\beta\alpha} \\ \mathbf{V}_{\beta\alpha}^T & \mathbf{V}_{\alpha} \end{pmatrix},$$

and

$$\mathbf{V}_{\beta} = \frac{1}{\sigma_{\epsilon}^2} \tilde{\mathbf{X}}^T \tilde{\mathbf{X}} + \mathbf{P}_{\lambda^*}, \quad \mathbf{V}_{\alpha} = \frac{1}{\sigma_{\epsilon}^2} \mathbf{Z}^T \mathbf{Z} + \boldsymbol{\Sigma}_{\alpha}^{-1}, \quad \mathbf{V}_{\beta\alpha} = \frac{1}{\sigma_{\epsilon}^2} \tilde{\mathbf{X}}^T \mathbf{Z}.$$

The proof of Theorem 3.1 is provided in Appendix A of the Supplemental Material. Theorem 3.1 establishes the joint Gaussian posterior distribution of $(\tilde{\boldsymbol{\beta}}, \boldsymbol{\alpha})$, whose block-structured precision matrix naturally suggests an iterative estimation scheme. Because both conditional posteriors— $p(\tilde{\boldsymbol{\beta}} | \boldsymbol{\alpha}, \mathbf{y})$ and $p(\boldsymbol{\alpha} | \tilde{\boldsymbol{\beta}}, \mathbf{y})$ —have closed-form Gaussian expressions, one can al-

ternately update the spline coefficients and random effects using their respective conditional expectations.

Theorem 3.1 tells us that the estimation problem can be organized into a blockwise update scheme: within each iteration, the updates for $(\tilde{\beta}, \alpha)$ are obtained by alternating their two closed-form conditional posteriors, while the variance components $(\Sigma_\alpha, \sigma_\epsilon^2)$ are updated in a separate step using their corresponding estimating equations or profile likelihoods. Treating the variance components as fixed *within each block update* yields a Gibbs-type iteration that converges to the joint posterior mode, and it is in this sense that the log-likelihood may be expressed compactly as $\ell(\tilde{\beta}, \alpha)$ during the inner updates. For clarity of exposition, we therefore adopt this simplified notation in place of the full joint likelihood in (2) when describing the blockwise updates.

Although this blockwise scheme is computationally convenient in the centralized setting, implementing it in distributed environments requires an additional insight: each update depends on quadratic forms such as $\tilde{\mathbf{X}}^\top \tilde{\mathbf{X}}$, $\tilde{\mathbf{X}}^\top \mathbf{Z}$, and $\mathbf{Z}^\top \mathbf{Z}$. These objects are potentially high-dimensional and cannot be communicated efficiently in raw form. The key observation is that these quantities can be expressed entirely through low-dimensional sufficient statistics. Theorem 3.2 formalizes this reduction by showing that the precise summaries needed for all conditional updates can be computed locally and aggregated without accessing raw data. This sufficient-statistics representation transforms the blockwise updates into a scalable and communication-efficient procedure that preserves full likelihood information in large-scale settings.

Theorem 3.2 (Sufficient Statistics for the VCMMs). *For each data partition $\mathcal{D}_k = (\mathbf{y}_k, \tilde{\mathbf{X}}_k, \mathbf{Z}_k)$,*

$k = 1, \dots, K$, compute the sufficient statistics

$$\boldsymbol{\Gamma}_k = \left\{ \begin{array}{l} a_k = \sum_{\ell=1}^{n_k} y_{k\ell}^2 \in \mathbb{R}, \\ \mathbf{b}_k = \sum_{\ell=1}^{n_k} y_{k\ell} \tilde{\mathbf{x}}_{k\ell} \in \mathbb{R}^{(p+1)Q}, \\ \mathbf{C}_k = \sum_{\ell=1}^{n_k} \tilde{\mathbf{x}}_{k\ell} \tilde{\mathbf{x}}_{k\ell}^\top \in \mathbb{R}^{(p+1)Q \times (p+1)Q}, \\ \mathbf{d}_k = \mathbf{Z}_k^\top \mathbf{y}_k \in \mathbb{R}^q, \\ \mathbf{B}_k = \tilde{\mathbf{X}}_k^\top \mathbf{Z}_k \in \mathbb{R}^{(p+1)Q \times q}, \\ \mathbf{H}_k = \mathbf{Z}_k^\top \mathbf{Z}_k \in \mathbb{R}^{q \times q} \end{array} \right\}.$$

Let the aggregated summaries be $\mathbf{C} = \sum_k \mathbf{C}_k$, $\mathbf{b} = \sum_k \mathbf{b}_k$, $\mathbf{B} = \sum_k \mathbf{B}_k$, $\mathbf{H} = \sum_k \mathbf{H}_k$, $\mathbf{d} = \sum_k \mathbf{d}_k$, $a = \sum_k a_k$, and $N = \sum_{k=1}^K n_k$. Then the model parameters can be estimated as

$$\begin{aligned} \hat{\boldsymbol{\beta}} &= (\mathbf{C} + \sigma_\epsilon^2 \mathbf{P}_{\lambda^*})^{-1} (\mathbf{b} - \mathbf{B} \hat{\boldsymbol{\alpha}}), & \hat{\boldsymbol{\alpha}} &= (\mathbf{H} + \sigma_\epsilon^2 \boldsymbol{\Sigma}_\alpha^{-1})^{-1} (\mathbf{d} - \mathbf{B}^\top \hat{\boldsymbol{\beta}}), \\ \hat{\sigma}_\epsilon^2 &= \frac{1}{N} \left[a - 2 \hat{\boldsymbol{\beta}}^\top \mathbf{b} + \hat{\boldsymbol{\beta}}^\top \mathbf{C} \hat{\boldsymbol{\beta}} - 2 \hat{\boldsymbol{\alpha}}^\top \mathbf{d} + 2 \hat{\boldsymbol{\beta}}^\top \mathbf{B} \hat{\boldsymbol{\alpha}} + \hat{\boldsymbol{\alpha}}^\top \mathbf{H} \hat{\boldsymbol{\alpha}} \right], & \hat{\boldsymbol{\Sigma}}_\alpha &= \frac{\hat{\boldsymbol{\alpha}} \hat{\boldsymbol{\alpha}}^\top}{q}. \end{aligned}$$

Theorem 3.2 demonstrates that all model parameters can be consistently estimated using only the local summaries $\boldsymbol{\Gamma}_k$ from each computational node or subdataset, without requiring access to raw data. The proof is provided in Appendix B of the Supplemental Material. Together, Theorems 3.1 and 3.2 establish the analytical foundation for iteratively updating the random effects $\boldsymbol{\alpha}$ and spline coefficients $\hat{\boldsymbol{\beta}}$. Each iteration applies the conditional posterior means implied by Theorem 3.1, with all quantities expressed through the aggregated sufficient statistics derived in Theorem 3.2. The resulting blockwise Gibbs-type procedure is summarized in Algorithm 1. Alternatively, estimation may be formulated using the marginal likelihood—obtained by integrating out $\boldsymbol{\alpha}$ —or via restricted maximum likelihood (REML), which adjusts for fixed-effect degrees of freedom to reduce small-sample bias (Patterson and Thompson, 1971). Under standard regularity conditions, the joint, marginal, and restricted

likelihood formulations yield asymptotically equivalent estimators for both fixed effects and variance components (Harville, 1977; Searle et al., 2009; McCulloch and Searle, 2004; Rao, 1971). Hence, in large-scale settings, the practical differences among these approaches are negligible.

Algorithm 1 Sufficient-Statistics-Based Distributed Estimation for VCMMs

- 1: Initialize $\tilde{\beta}^{(0)}, \alpha^{(0)}$
- 2: **for** each partition $k = 1, \dots, K$ **do**
- 3: Compute $a_k, \mathbf{b}_k, \mathbf{C}_k, \mathbf{d}_k, \mathbf{B}_k, \mathbf{H}_k$
- 4: **end for**
- 5: **for** $t = 1, \dots, T$ **do**
- 6: Update $\tilde{\beta}^{(t)}, \alpha^{(t)}$ using Theorem 3.2.
- 7: **end for**
- 8: **Output:** $\hat{\beta}, \hat{\alpha}, \hat{\sigma}_\epsilon^2, \hat{\Sigma}_\alpha$

Recent advances in scalable and randomized singular value decomposition (SVD) (Halko et al., 2011; Meng et al., 2014; Li et al., 2014; Cai et al., 2015; Liberty et al., 2007; Drineas et al., 2012) enable numerically stable computation even in massive, distributed environments. These techniques can be seamlessly integrated into the sufficient-statistics framework to enhance robustness when either $\sum_k \mathbf{C}_k$ or $\sum_k \mathbf{Z}_k^\top \mathbf{Z}_k$ is ill-conditioned. Define

$$\mathbf{G} = \mathbf{C} + \sigma_\epsilon^2 \mathbf{P}_{\lambda^*}, \quad \mathbf{H}_{\text{aug}} = \mathbf{H} + \sigma_\epsilon^2 \Sigma_\alpha^{-1}.$$

For clarity, throughout this section we reserve $\mathbf{H} = \sum_k \mathbf{H}_k$ for the aggregated random-effect Gram matrix and use $\mathbf{H}_{\text{aug}} = \mathbf{H} + \sigma_\epsilon^2 \Sigma_\alpha^{-1}$ for its ridge-augmented counterpart used in SVD stabilization. Then, we decompose

$$\mathbf{G} = \mathbf{U}_G \mathbf{S}_G \mathbf{V}_G^\top, \quad \mathbf{H}_{\text{aug}} = \mathbf{U}_H \mathbf{S}_H \mathbf{V}_H^\top.$$

The stabilized estimators are then given by

$$\hat{\beta} = \mathbf{V}_G \mathbf{S}_G^{-1} \mathbf{U}_G^\top \left(\sum_k \mathbf{b}_k - \sum_k \mathbf{B}_k \hat{\alpha} \right), \quad \hat{\alpha} = \mathbf{V}_H \mathbf{S}_H^{-1} \mathbf{U}_H^\top \left(\sum_k \mathbf{Z}_k^\top \mathbf{y}_k - \sum_k \mathbf{Z}_k^\top \tilde{\mathbf{X}}_k \hat{\beta} \right),$$

where $\mathbf{U}_H \mathbf{S}_H \mathbf{V}_H^\top$ is the SVD of \mathbf{H}_{aug} , and $\mathbf{B}_k = \tilde{\mathbf{X}}_k^\top \mathbf{Z}_k$ and $\mathbf{H}_k = \mathbf{Z}_k^\top \mathbf{Z}_k$ denote the local cross- and random-effect Gram matrices, respectively. As a result, Algorithm 1 can be naturally extended to a numerically stabilized version through adequate SVD usage, as described in Algorithm 2.

Algorithm 2 Distributed SVD–Stabilized Sufficient-Statistics Estimation for the VCMMs

- 1: Accumulate sufficient statistics across all partitions.
- 2: Compute $\mathbf{G} = \mathbf{C} + \sigma_\epsilon^2 \mathbf{P}_{\lambda^*}$ and $\mathbf{H}_{\text{aug}} = \mathbf{H} + \sigma_\epsilon^2 \mathbf{\Sigma}_\alpha^{-1}$, then perform large-scale SVD.
- 3: **for** $t = 1, \dots, T$ **do**
- 4: Update $\tilde{\boldsymbol{\beta}}^{(t)}, \boldsymbol{\alpha}^{(t)}$ using the SVD-based updates.
- 5: **end for**
- 6: **Output:** $\hat{\boldsymbol{\beta}}, \hat{\boldsymbol{\alpha}}, \hat{\sigma}_\epsilon^2, \hat{\mathbf{\Sigma}}_\alpha$

Building on this formulation, randomized SVD provides a powerful numerical enhancement for stabilizing matrix inversion in large-scale settings, particularly when high-dimensional spline expansions induce severe multicollinearity or near-singular penalized cross-product structures. By producing low-rank spectral approximations, randomized SVD reduces computational cost while improving numerical conditioning in distributed environments where only aggregated sufficient statistics are available. In contrast, classical linear mixed-model algorithms typically do not require such stabilization, as their mixed-model equations are sparse, block-structured, and involve only low-dimensional variance components, allowing efficient sparse Cholesky factorizations to fully exploit this structure. In the VCMM context, however, the Gram matrices are dense, high-dimensional, and aggregated across partitions, often becoming severely ill-conditioned. Randomized SVD mitigates these challenges while preserving scalability and communication efficiency, making this enhancement crucial for large-scale, high-dimensional varying-coefficient mixed models. Overall, this SVD-augmented formulation retains the scalability of the sufficient-statistics approach while ensuring numerical robustness under multicollinearity and near-singular design matrices, making it well-suited for modern distributed computation.

3.2 Theoretical Properties

A critical requirement for any iterative estimation procedure is the assurance of convergence to the correct solution. Without such guarantees, even computationally efficient algorithms may yield unreliable or unstable results in large-scale and high-dimensional settings. Building on the Gaussian posterior characterization in Section 3.1 (Theorem 3.1) and the sufficient-statistics formulation in Theorem 3.2, we establish the convergence properties of the proposed iterative estimators. Specifically, both Algorithm 1 (and its SVD-enhanced version Algorithm 2) are shown to converge to the unique posterior mode under mild regularity conditions. Furthermore, when interpreted in their stochastic (Gibbs) forms, the algorithms define ergodic Markov chains whose invariant distributions coincide with the exact joint posterior, ensuring both numerical stability and valid Bayesian uncertainty quantification.

Theorem 3.3 (Convergence of Algorithms 1 and 2). *Let $\{\tilde{\beta}^{(t)}, \alpha^{(t)}\}$ be generated by the iterative procedures described in Algorithms 1 and 2. Suppose Conditions (A1)–(A6) in Appendix C of the Supplemental Material hold. Then the following properties are satisfied:*

- (i) *Under Conditions (A1)–(A4), the block Gauss–Seidel updates applied to the posterior quadratic objective form a globally convergent sequence. The iterates $\{(\tilde{\beta}^{(t)}, \alpha^{(t)})\}$ converge to the unique posterior mode*

$$(\tilde{\beta}^*, \alpha^*) = \arg \max_{\tilde{\beta}, \alpha} \pi(\tilde{\beta}, \alpha \mid \mathbf{y}),$$

ensuring numerical stability and a well-defined sufficient-statistics estimator.

- (ii) *Under Conditions (A1)–(A3) and (A6), the alternating Gibbs sampler based on the two full conditional distributions of $(\tilde{\beta}, \alpha)$ is π -irreducible and aperiodic, with invariant distribution equal to the joint posterior*

$$\pi(\tilde{\beta}, \alpha \mid \mathbf{y}).$$

(iii) *For any integrable posterior functional ϕ , the Gibbs chain satisfies the strong law of large numbers:*

$$\frac{1}{T} \sum_{t=1}^T \phi(\tilde{\boldsymbol{\beta}}^{(t)}, \boldsymbol{\alpha}^{(t)}) \xrightarrow{a.s.} \mathbb{E}_\pi[\phi], \quad T \rightarrow \infty.$$

Consequently, empirical averages computed from the iterates consistently approximate posterior expectations.

The detailed proof of Theorem 3.3 is provided in Appendix D of the Supplemental Material. Intuitively, the result establishes three key facts about our iterative estimation procedure. First, when the updates are applied deterministically, the algorithm converges to the unique posterior mode, ensuring that the sufficient-statistics estimator is well-defined and numerically stable. Second, when the same updates are interpreted as alternating draws from the two full conditional distributions in Section 3.1, they define an ergodic Markov chain whose invariant distribution coincides with the exact joint posterior, enabling coherent Bayesian uncertainty quantification. Third, long-run empirical averages of any integrable posterior functional converge almost surely to their corresponding posterior expectations, guaranteeing valid Monte Carlo approximation. Together, these properties ensure both optimization consistency and statistical correctness, even in the presence of high-dimensional spline bases and large random-effect components.

While these theoretical guarantees validate the correctness of the iterative scheme, naively applying it on massive datasets is still computationally and communication intensive, particularly when data are distributed across machines or institutions. In such settings, repeatedly transmitting raw observations or forming full design matrices is infeasible. These considerations motivate the communication-efficient VCMM framework developed in the next section, which leverages low-dimensional sufficient statistics, randomized spectral stabilization, and distributed aggregation to enable exact likelihood-based inference without sharing raw data or incurring excessive communication overhead.

4 Communication-Efficient Distributed Estimation for VCMMs

While Section 3 develops the VCMM in an idealized centralized regime without communication constraints ($c = \infty$), practical difficulties arise when estimation must be carried out across multiple distributed nodes. Theorem 3.2 shows that the Gaussian VCMM likelihood (2) depends on each node’s data only through a fixed-dimensional collection of sufficient statistics. This structure suggests that, in principle, likelihood-based estimation might be achieved without transmitting raw observations or full spline design matrices. However, in distributed environments, several challenges remain: sufficient statistics must still be communicated across nodes; iterative procedures such as posterior block updates may require repeated exchange of information; and it is unclear whether naive use of these summaries alone can achieve optimal inference under a strict communication budget. These considerations motivate the development of communication-efficient methods that exploit the sufficient-statistics representation while minimizing the amount of information exchanged. A particularly promising strategy is the use of one-step estimators, which require only a single round of communication of fixed-dimensional summaries while retaining the asymptotic properties of the centralized estimator.

4.1 One-Step Estimation via Aggregated Sufficient Statistics

To simplify notation, we express the original objective function (3) solely in terms of the key model parameters $(\tilde{\beta}, \alpha)$. As Theorem 3.1 shows, these parameters admit closed-form conditional posteriors, enabling a blockwise update scheme in which $(\tilde{\beta}, \alpha)$ are alternately updated while the variance components $(\Sigma_\alpha, \sigma_\epsilon^2)$ are refined in a separate estimation step. Because the variance components are held fixed only *within each inner update* for $(\tilde{\beta}, \alpha)$, it is convenient during these updates to write the relevant objective succinctly as $\ell(\tilde{\beta}, \alpha)$, omitting constants involving the variance parameters. Under this notation, the communication-

constrained formulation becomes

$$(\hat{\tilde{\beta}}, \hat{\alpha}) = \arg \max_{\tilde{\beta}, \alpha} \ell(\tilde{\beta}, \alpha) \quad \text{subject to} \quad \text{total bits communicated} \leq cdk.$$

To implement this optimization in a distributed environment, suppose the full sample is partitioned into $\{\mathcal{D}_k\}_{k=1}^K$, where node k holds $(\mathbf{y}_k, \tilde{\mathbf{X}}_k, \mathbf{Z}_k)$ with n_k observations. Under the hierarchical formulation in (5), the log-likelihood decomposes additively across nodes as

$$\ell(\tilde{\beta}, \alpha) = \sum_{k=1}^K \ell_k(\tilde{\beta}, \alpha),$$

reflecting the conditional independence structure inherent to the VCMM. Directly maximizing this objective across distributed nodes would, however, require repeatedly transmitting large design matrices or high-dimensional intermediate quantities—an approach incompatible with the communication limit total bits communicated $\leq cdk$. These observations motivate a distributed estimation strategy that uses one-step updates built from low-dimensional sufficient statistics, described next.

To mitigate the communication burden while preserving likelihood-based inference, each node constructs a quadratic approximation of its local log-likelihood contribution around an initial pilot estimator $\boldsymbol{\theta}_0 = (\tilde{\beta}_0, \alpha_0)$:

$$\ell_k(\boldsymbol{\theta}) \approx \ell_k(\boldsymbol{\theta}_0) + \mathbf{s}_k(\boldsymbol{\theta}_0)^\top (\boldsymbol{\theta} - \boldsymbol{\theta}_0) - \frac{1}{2} (\boldsymbol{\theta} - \boldsymbol{\theta}_0)^\top \mathbf{I}_k(\boldsymbol{\theta}_0) (\boldsymbol{\theta} - \boldsymbol{\theta}_0),$$

where $\mathbf{s}_k(\boldsymbol{\theta}_0)$ is the local score and $\mathbf{I}_k(\boldsymbol{\theta}_0)$ is the observed information. Summing these local surrogates yields a global quadratic objective whose maximizer requires transmitting only fixed-dimensional gradient and curvature terms, rather than raw observations.

Aggregating node-wise contributions leads immediately to the *one-step* Newton update

$$\boldsymbol{\theta}^{(1)} = \boldsymbol{\theta}_0 + \mathbf{I}(\boldsymbol{\theta}_0)^{-1} \mathbf{S}(\boldsymbol{\theta}_0), \quad (7)$$

where

$$\mathbf{S}(\boldsymbol{\theta}_0) = \sum_{k=1}^K \mathbf{s}_k(\boldsymbol{\theta}_0), \quad \mathbf{I}(\boldsymbol{\theta}_0) = \sum_{k=1}^K \mathbf{I}_k(\boldsymbol{\theta}_0).$$

When the pilot $\boldsymbol{\theta}_0$ is \sqrt{N} -consistent—e.g., obtained from a single node—this update is asymptotically equivalent to the fully centralized maximizer. Crucially, its computation requires only aggregated gradient and information terms, both of which have dimension independent of the local sample sizes n_k .

While (7) already enables communication-efficient inference, directly forming node-wise gradients and Hessians may still require transmitting high-dimensional design matrices $(\tilde{\mathbf{X}}_k, \mathbf{Z}_k)$ or repeatedly evaluating local likelihood contributions. Fortunately, under the Gaussian VCMM introduced in Section 3, each node’s likelihood depends on its data only through a fixed set of low-dimensional *sufficient statistics*. These summaries compress the contribution of n_k observations into quantities whose dimensions depend solely on the model complexity—namely, the spline basis dimension $(p+1)Q$ and the random-effect dimension q —but not on n_k itself. Consequently, the one-step update can be computed using only aggregated sufficient statistics, further reducing communication while preserving full likelihood information. The following theorem provides explicit closed-form expressions for the one-step estimator in terms of these aggregated summaries.

Theorem 4.1 (One-Step Estimation via Sufficient Statistics). *Let $\boldsymbol{\theta} = (\tilde{\boldsymbol{\beta}}, \boldsymbol{\alpha})$ and suppose an initial estimator $\boldsymbol{\theta}_0 = (\tilde{\boldsymbol{\beta}}_0, \boldsymbol{\alpha}_0)$ is computed from one local node using its sufficient statistics. Define the aggregated summaries*

$$\mathbf{C} = \sum_{k=1}^K \mathbf{C}_k, \quad \mathbf{b} = \sum_{k=1}^K \mathbf{b}_k, \quad \mathbf{B} = \sum_{k=1}^K \mathbf{B}_k, \quad \mathbf{H} = \sum_{k=1}^K \mathbf{H}_k, \quad \mathbf{d} = \sum_{k=1}^K \mathbf{d}_k, \quad a = \sum_{k=1}^K a_k.$$

Then the one-step estimator based on aggregated sufficient statistics is

$$\boldsymbol{\theta}^{(1)} = \boldsymbol{\theta}_0 - \mathbf{K}_1^{-1} \mathbf{g}(\boldsymbol{\theta}_0),$$

where the global gradient is given by

$$\mathbf{g}_{\tilde{\beta}}(\boldsymbol{\theta}_0) = \frac{1}{\sigma_\epsilon^2} \left(\mathbf{C} \tilde{\beta}_0 + \mathbf{B} \boldsymbol{\alpha}_0 - \mathbf{b} \right) + \mathbf{P}_{\lambda^*} \tilde{\beta}_0, \quad \mathbf{g}_{\boldsymbol{\alpha}}(\boldsymbol{\theta}_0) = \frac{1}{\sigma_\epsilon^2} \left(\mathbf{B}^\top \tilde{\beta}_0 + \mathbf{H} \boldsymbol{\alpha}_0 - \mathbf{d} \right) + \boldsymbol{\Sigma}_{\boldsymbol{\alpha}}^{-1} \boldsymbol{\alpha}_0.$$

The pivot Hessian from a reference node (say node 1) is

$$\mathbf{K}_1 = \begin{pmatrix} \frac{1}{\sigma_\epsilon^2} \mathbf{C}_1 + \mathbf{P}_{\lambda^*} & \frac{1}{\sigma_\epsilon^2} \mathbf{B}_1 \\ \frac{1}{\sigma_\epsilon^2} \mathbf{B}_1^\top & \frac{1}{\sigma_\epsilon^2} \mathbf{H}_1 + \boldsymbol{\Sigma}_{\boldsymbol{\alpha}}^{-1} \end{pmatrix}.$$

The variance component is updated as

$$\hat{\sigma}_\epsilon^2 = \frac{1}{N} \left[a - 2 \tilde{\beta}^{(1)\top} \mathbf{b} + \tilde{\beta}^{(1)\top} \mathbf{C} \tilde{\beta}^{(1)} - 2 \boldsymbol{\alpha}^{(1)\top} \mathbf{d} + 2 \tilde{\beta}^{(1)\top} \mathbf{B} \boldsymbol{\alpha}^{(1)} + \boldsymbol{\alpha}^{(1)\top} \mathbf{H} \boldsymbol{\alpha}^{(1)} \right]. \quad (8)$$

A detailed proof of Theorem 4.1 is provided in Appendix E of the Supplemental Material. Note that this conditional factorization property is standard in hierarchical Gaussian models and underpins distributed inference for generalized linear mixed models (Zhang and Lin, 2004). More general patterns of cross-node residual correlation can be accommodated by extending the random-effect covariance structure (e.g., introducing spatially indexed random effects, temporal autoregressive components, or separable spatiotemporal kernels), without altering the sufficient-statistics interface. Such extensions preserve the algebraic form of the conditional likelihood and therefore do not affect the communication complexity of the proposed framework.

Theorem 4.1 highlights several key features of the proposed approach. First, for Gaussian VCMMs, the local log-likelihood depends on the observed data only through a fixed set of sufficient statistics, allowing each node to compress its contribution without loss of information. Second, once these summaries are aggregated, the resulting global score and information match those of the centralized estimator up to $O_p(1/\sqrt{N})$, ensuring that the one-step update preserves the same local curvature and optimization direction as a full Newton

iteration on the pooled data. Finally, under standard regularity conditions, this guarantees that $\boldsymbol{\theta}^{(1)}$ is asymptotically equivalent to the centralized MLE, providing first-order statistical efficiency while requiring only a single round of communication. When the aggregated cross-product matrices exhibit near-singularity, an SVD-based stabilization can be incorporated without increasing communication cost. Details of the SVD implementation are discussed in Appendix F of the Supplemental Material.

The use of sufficient statistics ensures that the communication cost per node remains constant regardless of n_k , while still preserving full statistical information for estimation. Moreover, the one-step update provides an efficient bridge between *distributed computation* and *likelihood-based inference*, yielding estimators that are both communication-efficient and theoretically justified for large-scale VCMM estimation. While this establishes practical feasibility, it also raises important questions about correctness, convergence, and stability of the resulting procedure. The next subsection addresses these issues by establishing asymptotic and non-asymptotic guarantees for the one-step estimator.

4.2 Theoretical Properties of the Communication-Efficient Estimator

This subsection establishes both asymptotic and non-asymptotic properties of the proposed one-step estimator defined in Theorem 4.1. The results accommodate dependence structures that commonly arise in large-scale migration settings—including clustered, longitudinal, and spatial correlation—thereby extending standard communication-efficient inference frameworks that typically assume independence across observations or nodes.

Theorem 4.2 (Asymptotic Efficiency of the One Step Estimator under Dependent Data). *Under Conditions (B1)–(B4) in Appendix G of the Supplemental Material, the one-step*

estimator $(\tilde{\beta}^{(1)}, \alpha^{(1)})$ obtained from Theorem 4.1 satisfies

$$\sqrt{N} \begin{pmatrix} \tilde{\beta}^{(1)} - \tilde{\beta}^* \\ \alpha^{(1)} - \alpha^* \end{pmatrix} \xrightarrow{d} N(0, \mathcal{I}^{-1}),$$

where \mathcal{I} denotes the centralized Fisher information matrix accounting for both fixed- and random-effect contributions as well as the dependence structure.

Corollary 4.3 (Efficiency Equivalence with the Centralized MLE). *Under Conditions (B1)–(B4), the one-step estimator obtained from Theorem 4.1 attains the same first-order asymptotic efficiency as the centralized maximum likelihood estimator, despite operating under fixed communication constraints.*

Detailed proofs of Theorem 4.2 and Corollary 4.3 are provided in Appendix H of the Supplemental Material. Prior work, such as Jordan et al. (2019), demonstrates that communication-efficient one-step estimators can attain full asymptotic efficiency in i.i.d. settings. Theorem 4.2 broadens this result to settings with structured dependence—including spatial, clustered, and longitudinal migration flows—by exploiting the sufficiency of the aggregated summaries $(a, \mathbf{b}, \mathbf{C}, \mathbf{d}, \mathbf{B}, \mathbf{H})$ introduced in Theorem 4.1. This guarantees that no information relevant to estimation is lost through distributed aggregation, even in the presence of cross-unit dependence, thereby preserving the same local curvature and Fisher information as the centralized likelihood. As a result, the one-step estimator maintains first-order statistical efficiency across a broad class of correlated data environments.

Theorem 4.4 (Non-Asymptotic Analysis of the One Step Estimator). *Under Conditions (B1) and (B3)–(B6) in Appendix G of the Supplemental Material, for any $t > 0$,*

$$\Pr\left(\left\|\frac{1}{K} \sum_{k=1}^K \mathbf{C}_k - \mathbb{E}[\mathbf{C}_k]\right\| \geq t\right) \leq 2((p+1)Q)^2 \exp\left(-\frac{cKt^2}{\varsigma^2 + C_x^2 t}\right), \quad (9)$$

for constants $c > 0$, $\varsigma > 0$, and $C_x > 0$, with analogous bounds holding for \mathbf{b}_k , \mathbf{d}_k , \mathbf{B}_k , and \mathbf{H}_k . Because the mapping from aggregated summaries to $(\tilde{\beta}^{(1)}, \alpha^{(1)})$ in Theorem 4.1

is locally Lipschitz in a neighborhood of $\boldsymbol{\theta}^*$, these concentration bounds yield corresponding high-probability finite-sample guarantees for the one-step estimator.

The proof of Theorem 4.4 is provided in Appendix I of the Supplemental Material. The sufficient statistics used in Theorem 4.1 preserve all Fisher information about the parameter vector $\boldsymbol{\theta} = (\tilde{\boldsymbol{\beta}}, \boldsymbol{\alpha})$, and, under completeness, any unbiased estimator constructed from them attains uniformly minimum variance by the Lehmann–Scheff   theorem. Within the distributed VCMM, these properties imply that the resulting one-step update is not only communication-optimal—requiring fixed message dimension per node—but also variance-optimal among unbiased estimators, even in the presence of dependence across partitions. Together with the asymptotic guarantees established above, these results provide a rigorous foundation for the use of aggregated summaries in large-scale distributed inference.

While these theoretical properties ensure correctness, stability, and efficiency of the proposed estimator, it remains important to assess its practical behavior under realistic migration-like data regimes. In the next section, we conduct a series of numerical simulations to evaluate the properties.

5 Numerical Studies

We design four simulation experiments that progressively increase in model complexity to demonstrate the flexibility and robustness of the proposed distributed VCMM framework. These examples mirror the structural challenges encountered in real data analyses and jointly evaluate the statistical accuracy and computational scalability of the proposed estimators. The first experiment examines a simple varying-coefficient mixed model for which the full-data centralized estimator is available. This setting allows us to validate the exact recoverability of the sufficient-statistics (SS) estimator from Algorithm 1, thereby confirming the theoretical property established in Theorem 3.2 and Section 3. The second experiment studies the SVD-stabilized estimator in high-dimensional random-effect settings,

assessing numerical stability when the random-effects structure becomes dense and correlated—a common feature of spatiotemporal applications. The third experiment compares three approaches—the direct estimator, the SS estimator introduced in Section 2, and the one-step (OS) composite sufficient likelihood estimator developed in Section 4. This example focuses on large-scale settings and evaluates both statistical fidelity and computational gains under communication constraints. Finally, the fourth experiment extends the framework to a two-dimensional smooth-surface model, where multiple varying coefficients interact across dimensions, mimicking the complex functional structure observed in real-world migration and environmental datasets. Across all experiments, we describe the simulation design, report parameter estimation accuracy, evaluate surface recovery performance, and quantify computational efficiency. Together, these studies highlight the advantages of the proposed SS and OS estimators in both accuracy and scalability.

5.1 Example 1: Validation of the Sufficient-Statistics-Based Estimation

We begin by validating the sufficient-statistics property established in Theorem 3.2 using a simple varying-coefficient mixed model for which the centralized full-data estimator can be computed explicitly. This experiment is designed to verify that the SS-based estimator from Algorithm 1 exactly reproduces the conventional estimator, as guaranteed by theory, while offering significant computational savings. Specifically, we simulate data from model (1): $y_i = \beta_0 + \beta_1(t_i)X_i + \alpha + \epsilon_i$, where $\beta_1(t) = \sin(2\pi t)$, $t_i \sim \text{Uniform}(0, 1)$, $X_i \sim \text{Uniform}(0, 1)$, $\beta_0 = 2.0$, and $\alpha \sim N(0, \sigma_\alpha^2)$. Nineteen cubic B-spline basis functions are used to approximate $\beta_1(t)$, and basis orthogonalization ensures strong numerical stability. The smoothing parameter is selected via cross-validation. We generate $N = 1,000$ observations and repeat the experiment over 100 Monte Carlo replications. This design mirrors the dimensional structure of our real data while remaining small enough to allow exact comparison with centralized estimation.

Table 1 summarizes the results. The correlations between the SS estimator and the conventional estimator exceed 0.99 for all components, indicating numerical equivalence up to machine precision. The MSEs with respect to the true parameters are essentially identical, confirming the theoretical result of Theorem 3.2: the SS-based procedure yields exactly the same estimates as the full-data maximum likelihood estimator. The computational advantage, however, is substantial. Because the SS estimator replaces the raw data with compact summary matrices, it eliminates repeated passes through the dataset and dramatically reduces memory usage and communication cost. As sample size or model complexity increases, this reduction becomes increasingly pronounced, enabling large-scale estimation to remain fully efficient while avoiding the bottlenecks of centralized computation. Overall, Example 1 confirms that the SS formulation retains complete statistical fidelity while providing strong computational benefits, forming the foundation for the more complex scenarios explored in subsequent examples.

Table 1: Comparison of estimation accuracy between sufficient-statistics (SS) and conventional estimators under Example 1.

	β_0	$\beta_1(t)$	σ_α^2
Correlation (SS vs Conventional)	0.999	0.998	0.9999
MSE (SS method)	0.001	0.038	0.006
MSE (Conventional method)	0.001	0.020	0.005

5.2 Example 2: High-Dimensional Random Effects with SVD Stabilization

To further assess the robustness of the proposed framework in settings with highly complex random-effect structures, we extend the simulation design to a high-dimensional scenario and evaluate the SVD-stabilized estimator of Algorithm 2. This setting mirrors challenges commonly encountered in large-scale spatiotemporal applications—including migration modeling—where random effects encode dependence across numerous origins, destinations, and temporal components, often resulting in severely ill-conditioned Gram matrices.

We simulate data from model (1) with a 200-dimensional random-effects vector $\boldsymbol{\alpha} \sim N(\mathbf{0}, \boldsymbol{\Sigma}_\alpha)$, where $\boldsymbol{\Sigma}_\alpha$ induces mild adjacent correlations, specifically $\text{Corr}(\alpha_i, \alpha_{i+1}) = 0.1$. This design captures the complexity of large migration datasets while maintaining full control over the covariance structure. A detailed description of the random-effects design matrix \mathbf{Z} and the construction of $\boldsymbol{\Sigma}_\alpha$ is provided in Appendix J of the Supplemental Material. In the setting, the empirical Gram matrices $\mathbf{C} = \tilde{\mathbf{X}}^\top \tilde{\mathbf{X}}$ and $\mathbf{H} = \mathbf{Z}^\top \mathbf{Z}$ become nearly singular, causing substantial numerical instability in naive matrix inversion. To address this, we compare two stabilized one-step estimation schemes: (i) a conventional VCMM with full SVD-based estimator and (ii) the proposed method in Algorithm 2, which uses truncated eigendecomposition to approximate only the leading spectral components that govern curvature. Both estimators are implemented under the same initialization, smoothing parameters, and noise settings, allowing a direct comparison of statistical and numerical performance.

Table 2: Comparison between the proposed estimator in Algorithm 2 and the conventional estimator based on Example 2. Recorded values represent the average (standard deviation) across all replications.

Measurement	Proposed Method	Conventional Method
(A) Precision		
Reconstruction Error	5.6×10^{-2} (1.4 $\times 10^{-2}$)	2.2×10^{-13} (4.4 $\times 10^{-14}$)
Mean Squared Error (MSE)	0.449 (0.015)	0.451 (0.015)
(B) Correlation		
$\hat{\beta}_t$ Correlation	1.000 (8.7 $\times 10^{-6}$)	
$\hat{\alpha}$ Correlation	0.968 (0.011)	

Table 2 summarizes the results. The proposed SVD-stabilized estimator achieves nearly identical statistical performance to the full SVD estimator. The mean squared errors are indistinguishable, and the recovered coefficient function $\hat{\beta}_t$ agrees almost perfectly across the two methods ($\text{corr} \approx 1$). The slightly larger reconstruction error observed for the proposed method reflects the truncation of small eigencomponents—components that contribute minimally to the curvature of the likelihood but whose removal substantially improves numerical

stability and computational scalability. The estimated random effects also remain highly correlated between the two estimators ($\text{corr} = 0.97$), confirming that the essential posterior structure is preserved. Taken together, these results demonstrate that the SVD-stabilized one-step estimator maintains first-order efficiency and numerical reliability even under severe ill-conditioning. By exploiting truncated spectral decomposition, the proposed method provides a scalable, stable, and computationally efficient alternative to full SVD, making it particularly suitable for large-scale distributed mixed-model estimation.

5.3 Example 3: Large-Sample Comparison of Direct, SS, and One-Step (OS) Estimation Methods

We further compare the SS method introduced in Section 3 and the OS estimator developed in Section 4 under a large-sample setting. The simulation follows the same model specification as in Example 1 but increases the sample size to $N = 10,000$. This design enables an evaluation of both statistical accuracy and computational scalability relative to the centralized direct estimator. All tuning parameters are chosen via cross-validation, and results are averaged over 100 replications.

As shown in Table 3, the SS and OS estimators produce parameter estimates that are nearly indistinguishable from those of the direct method. Correlations between the estimated parameters across all methods exceed 0.99, indicating that both SS and OS preserve the statistical information contained in the full dataset. Mean squared errors relative to the true parameters remain small and comparable across methods, demonstrating that neither approach sacrifices estimation accuracy. Predictive performance also remains consistent: training and testing errors for the varying coefficient $\beta_1(t)$ differ only within typical Monte Carlo variation, and prediction errors for the random-effects components follow the same pattern. Thus, both SS and OS maintain full inferential fidelity even at substantially larger sample sizes.

Panel (b) of Table 3 reports computational performance. At $N = 10,000$, the SS estima-

tor achieves an order-of-magnitude reduction in runtime compared with the direct method by replacing raw data with compact sufficient statistics. The OS estimator provides an additional dramatic improvement: a single refinement step reduces the number of iterations from tens to only a few, yielding more than four orders of magnitude speedup relative to the direct estimator. These scaling patterns highlight both the numerical stability and the practical efficiency of the proposed one-step refinement.

Table 3: Large-sample comparison of the SS and OS estimators. Results are based on Simulation Example 3. Panel (a) reports estimation accuracy, and Panel (b) reports computational efficiency. Recorded values are the average (standard deviation) across all replications.

(a) Estimation Accuracy		
	SS	OS
MSE of $\hat{\beta}_0$ (True = 2.00)	0.0002 (0.0004)	0.0002 (0.0004)
MSE of $\hat{\sigma}_{\alpha_1}^2$ (True = 0.2500)	0.0084 (0.0031)	0.0625 (0.0001)
MSE of $\hat{\sigma}_{\alpha_2}^2$ (True = 0.2500)	0.0083 (0.0032)	0.0625 (0.0001)
Training MSE ($\beta_1(t)$)	0.2334 (0.1546)	0.2334 (0.1547)
Test MSPE ($\beta_1(t)$)	0.1268 (0.0974)	0.1268 (0.0974)
MSPE (α_1)	0.0000 (0.0000)	0.0002 (0.0003)
MSPE (α_2)	0.0000 (0.0000)	0.0002 (0.0002)

(b) Computational Efficiency		
	SS	OS
Total Time (s)	8.5479 (2.4999)	0.0031 (0.0099)
Speedup (Relative to Direct)	3.3200x	9257.9700x

Overall, this large-sample experiment confirms that the SS and OS estimators match the direct estimator in statistical accuracy while offering substantial gains in computational efficiency. The OS method, in particular, converges rapidly—requiring only two iterations—making it especially attractive for large-scale applications.

5.4 Example 4: Two-Dimensional Varying-Coefficient Surface Models

We finally examine a two-dimensional varying-coefficient model to assess how the sufficient-statistics (SS) estimator scales to higher-dimensional smooth-surface settings. The coefficient surface is defined as $\beta_1(t_1, t_2) = \sin(2\pi(t_1 + t_2))$, where $(t_1, t_2) \in [0, 1]^2$ and a total of $N = 10,000$ observations are generated. A tensor-product B-spline basis with $12 \times 12 = 144$ functions is used, representing a substantial increase in basis dimensionality relative to the one-dimensional case. The smoothing parameter is chosen via cross-validation, and the basis is orthogonalized to ensure numerical stability. This experiment evaluates estimation accuracy and computational scalability of the SS estimator relative to the traditional full-data estimator in a genuinely high-dimensional setting.

Table 4 reports the results. Both the traditional method and the SS estimator recover the underlying parameters with high accuracy, and the training and testing errors for the coefficient surface are essentially indistinguishable across the two approaches. Prediction errors for the random-effects components also agree closely, confirming that the SS reduction preserves all statistical information relevant for mixed-model estimation. These findings demonstrate that the SS approach maintains full statistical fidelity even as the basis dimensionality becomes large.

The computational gains are substantial. As shown in Table 4(b), the traditional estimator incurs a significantly higher runtime due to repeated operations on the large tensor-product design. In contrast, the SS formulation reduces computation time by more than an order of magnitude by replacing raw data with compact aggregated matrices. This example confirms that the SS framework scales effectively to two-dimensional smooth-surface models, maintaining accuracy while delivering dramatic improvements in computational efficiency.

Table 4: Two-dimensional varying-coefficient surface model: Results are based on Simulation Example 4. Panel (a) reports estimation accuracy for the traditional and SS methods, and Panel (b) summarizes computational efficiency. Recorded values are the average (standard deviation) across all replications.

(a) Estimation Accuracy		
	Traditional Method	SS
MSE of $\hat{\beta}_0$ (True = 2.00)	0.0006 (0.0009)	0.0006 (0.0009)
MSE of $\hat{\sigma}_\alpha^2$ (True = 0.25)	0.0544 (0.0010)	0.0545 (0.0010)
MSE of $\hat{\sigma}_\varepsilon^2$ (True = 0.0625)	0.0336 (0.0036)	0.0341 (0.0039)
Training MSE ($\beta_1(t_1, t_2)$)	0.0225 (0.0040)	0.0229 (0.0042)
Test MSPE ($\beta_1(t_1, t_2)$)	0.0225 (0.0041)	0.0228 (0.0042)
MSPE (α_1)	0.0009 (0.0002)	0.0009 (0.0002)
MSPE (α_2)	0.0792 (0.0012)	0.0792 (0.0012)

(b) Computational Efficiency		
	Traditional Method	SS
Total Time (s)	13.7941 (3.5419)	0.3578 (0.0798)
Speedup (Relative to Direct)	1.0000 (baseline)	38.5840 (3.4276)

In this complex two-dimensional setting, the SS estimator produces results virtually identical to the traditional full-data estimator while achieving more than an order-of-magnitude reduction in computation time. This confirms that the proposed sufficient-statistics framework scales efficiently to high-dimensional smooth-surface models without sacrificing statistical accuracy.

6 Real Data Application: Large-Scale Migration Analysis

A major empirical challenge in studying modern migration is that the data is inherently decentralized and computationally demanding. Through the extensive efforts of domain experts, a central empirical resource for U.S. internal migration research is now available in the dataset compiled by Habans and Douthat (2024), which consolidates multiple federal, state, and local migration records into a unified and publicly accessible platform. The full

collection, totaling approximately 1 TB and containing billions of individual records, provides one of the most comprehensive and fine-grained views of U.S. mobility patterns to date. Although these raw sources have been harmonized, the resulting dataset remains extremely large, covering two decades (2000–2020) of origin–destination flows, socioeconomic covariates, and environmental indicators across hundreds of Commuting Zones (CZs). Because of this scale, the data must be preprocessed, partitioned, and analyzed across multiple high-performance computing nodes. When the VCMM in equation (1) is applied, the associated spline design matrices for time-varying coefficients and the hierarchical random-effect structures quickly exceed the memory capacity of any single compute node. Transferring these matrices or centralizing raw data is infeasible, creating a genuine communication bottleneck for traditional likelihood-based mixed-model estimation. These computational and communication constraints directly motivate the use of the communication-efficient one-step (OS) sufficient-statistics estimator introduced in Section 4, which enables full-likelihood inference using only low-dimensional summary matrices computed locally on each node. Even in environments equipped with advanced supercomputing infrastructure, the proposed method remains advantageous by minimizing communication overhead, reducing memory pressure, and enabling scalable likelihood-based analysis without moving or replicating massive raw datasets.

To analyze the temporal and spatial structure of U.S. migration flows, we employ the VCMM

$$y_{ijt} = \beta_0(t) + \beta_1(t) \text{DisasterDeclarations}_{ijt} + \mathbf{Z}_{ijt}^\top \boldsymbol{\alpha} + \varepsilon_{ijt}, \quad (10)$$

where $\beta_0(t)$ denotes the time-varying baseline migration rate, $\beta_1(t)$ captures the evolving influence of federally declared disasters, and the random-effects term $\mathbf{Z}_{ijt}^\top \boldsymbol{\alpha}$ models structured spatial heterogeneity. The vector $\boldsymbol{\alpha}$ contains one “origin” effect and one “destination” effect for each CZ, yielding 308 random-effect parameters. The design matrix \mathbf{Z}_{ijt} is constructed so that each flow from origin i to destination j activates exactly two entries: one in the origin column and one in the destination column. The origin-associated component represents

outward migration pressure, or a *push effect*, while the destination-associated component represents in-migration attractiveness, or a *pull effect*. Because every origin–destination flow depends simultaneously on both terms, model (10) provides a principled mechanism for decomposing migration patterns into time-varying fixed effects and spatially varying push–pull forces. The temporal evolution of $\beta_0(t)$ and $\beta_1(t)$ is examined in Subsection 6.1, while the estimated push and pull effects are analyzed in detail in Subsection 6.2.

6.1 Exploration of Time-Varying Coefficients

This subsection focuses on the estimation of the time-varying coefficient functions in model (10). The temporal components, $\beta_0(t)$ and $\beta_1(t)$, are represented using cubic B-spline basis functions with 58 knot placement, allowing the model to capture long-run trends and short-run fluctuations while preserving numerical stability. Estimation is carried out using the OS sufficient-statistics procedure, which computes and aggregates low-dimensional summaries across distributed data batches, thereby avoiding transmission of raw migration records and enabling scalable inference on the full dataset.

As shown in Figure 1, the estimated functions $\beta_0(t)$ and $\beta_1(t)$ reveal clear and interpretable temporal dynamics. The baseline migration rate, $\beta_0(t)$, follows a cyclical pattern aligned with national economic conditions—peaking around 2002 during the post–tech boom period, rising again near 2010 following the Great Recession, and reaching another local maximum around 2015 before trending downward toward 2019. The narrow 95% confidence bands reflect high precision throughout the time domain, indicating that both long-term and short-term components are reliably captured.

The disaster-related effect, $\beta_1(t)$, exhibits modest yet statistically significant variation over the two decades. The effect is lowest around 2005–2006, coinciding with Hurricane Katrina and widespread Gulf Coast displacement, and increases steadily through 2010–2014 during successive cycles of disaster declarations and regional rebuilding. After 2015, the effect declines, suggesting growing local retention and adaptation capacity in disaster-prone

regions. The uniformly tight confidence intervals confirm that these temporal changes are well estimated and substantively meaningful. Additional insights into regional heterogeneity arise from the push and pull effects embedded in α , which are examined in detail in Section 6.2.

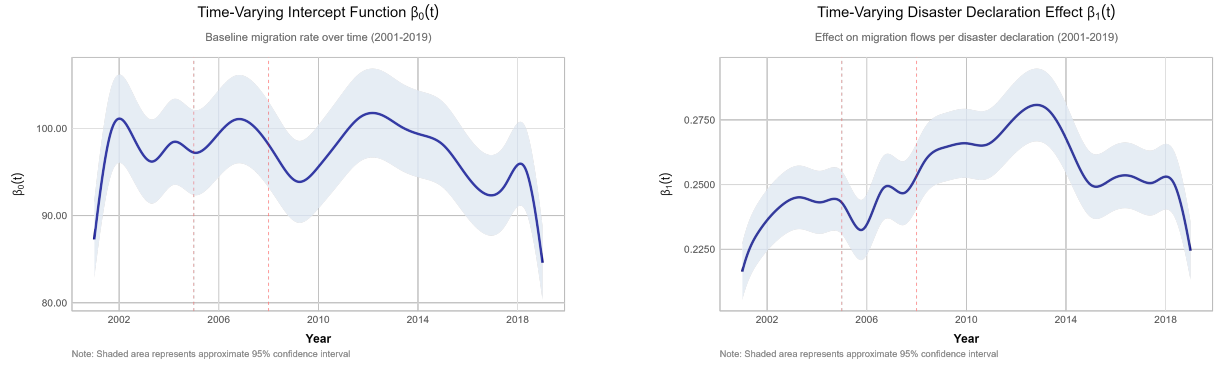


Figure 1: Estimated time-varying coefficient functions: (Left) baseline migration rate $\beta_0(t)$ from 2000–2020; (Right) disaster-declaration effect $\beta_1(t)$ capturing evolving disaster–migration dynamics. Shaded regions denote 95% confidence intervals.

6.2 Push and Pull Effects

In the VCMM specification (10), the random-effects structure naturally decomposes into two interpretable components: an *origin-specific* effect that captures outward migration pressure (a “push” effect) and a *destination-specific* effect that reflects the attractiveness of receiving regions (a “pull” effect). The estimated push and pull effects from the propsoed method reveal a clear spatial structure in migration dynamics across the United States. Across 154 CZs, destination (pull) effects range from approximately -85.538 to 345.149 , while origin (push) effects span from about -116.426 to 116.779 , indicating substantial heterogeneity in both in-migration appeal and out-migration pressure. The strong positive correlation between pull and push (0.607) suggests that regions capable of attracting newcomers also tend to exhibit higher outward mobility—characteristic of high-turnover, opportunity-driven labor markets. Major metropolitan areas dominate these patterns: Houston exhibits the strongest pull (345.149) alongside moderate push (26.309), and New Orleans shows both

a large pull (229.122) and the highest push value (116.779), consistent with its dynamic labor market and post-disaster population turnover. In contrast, smaller inland CZs such as Brady (-85.538) and Corsicana (-84.863) show persistently low attractivity, reflecting weaker economic diversification and peripheral geographic positioning.

Within Louisiana, the random-effects estimates highlight how environmental exposure and infrastructure capacity jointly shape migration behavior. Despite recurrent hurricane impacts and coastal vulnerabilities, New Orleans remains one of the strongest migration attractors in the country, underscoring its economic and cultural centrality. Its elevated push effect signals ongoing resident turnover driven by rebuilding cycles, housing constraints, and climate-induced mobility. Baton Rouge, by contrast, displays a modest push (-4.400) and functions as a regional stabilizer, absorbing migration from coastal parishes such as Terrebonne and Plaquemines. Together, these patterns portray Louisiana as a system in transition: environmental shocks generating outward movement from coastal CZs simultaneously enhance the pull of inland and metropolitan areas. Compared with traditional gravity models (e.g., Porojan (2001)), the VCMM random-effects formulation provides a sharper, more interpretable decomposition of spatially varying pull-push forces. The model identifies post-disaster recovery centers—such as New Orleans and Baton Rouge—and emerging inland attractors such as Lafayette and Alexandria, offering data-driven insight into climate adaptation and regional redistribution.

To further illustrate these dynamics, Figure 2 highlights patterns across southern and coastal states. Origin (emigration) and destination (immigration) random effects exhibit strong geographic clustering along the Gulf Coast and southeastern seaboard. Coastal states such as Louisiana and Florida maintain high destination effects (approximately +60 to +85) with moderate push, reflecting their persistent ability to attract residents despite climate exposure. South Carolina displays the largest net gain (+93.2), consistent with recent population inflows driven by coastal redevelopment, tourism growth, and the post-2010 housing recovery. In contrast, inland states such as New Mexico and Oklahoma show net losses

(−27.7 and below), reflecting sustained outmigration toward metropolitan corridors in Texas and Florida.

These patterns underscore the duality of coastal migration: regions exposed to environmental risk often remain powerful economic magnets. Louisiana maintains positive net inflow despite recurring storms, demonstrating a reconstruction-driven cycle of in-migration. Florida's strong inflow reinforces its role as a long-term population hub, balancing climate risk with labor-market opportunities and infrastructure investment. Conversely, inland areas with limited economic diversification—such as Oklahoma and New Mexico—show persistent outmigration, indicating that long-term population shifts depend more on regional resilience and economic opportunity than on hazard exposure alone. Overall, the push–pull decomposition reveals a dynamic migration equilibrium in which environmental stress, economic incentives, and adaptive capacity jointly shape population redistribution across the southern United States.

Migration Dynamics Across Southern U.S. States

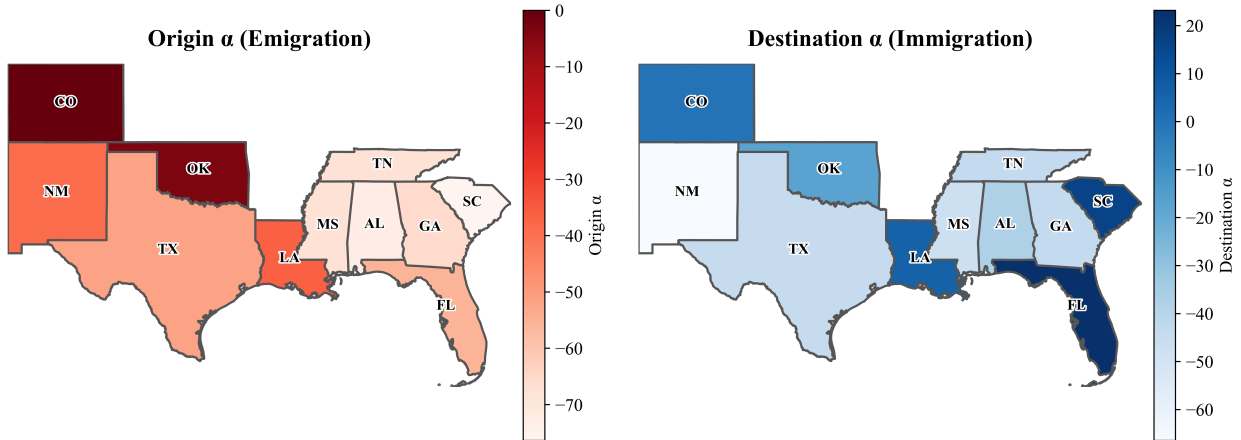


Figure 2: Southern States migration effects based on estimated random effects: (Left) origin α (push/emigration), (Center) destination α (pull/immigration), and (Right) net migration. Blue shading indicates positive in-migration (pull) and red indicates out-migration (push).

7 Summary and Future Directions

This paper develops a unified methodological framework for varying coefficient mixed models that accommodates both centralized and distributed large-scale settings with theoretical guarantees. In the unconstrained regime, we show that penalized spline estimators admit an exact bayesian hierarchical interpretation, yielding a full-information likelihood whose structure guarantees classical convergence rates and statistical optimality. Building on this representation, we identify a fixed, low-dimensional set of complete sufficient statistics that fully encodes each node’s likelihood contribution, thereby enabling a communication-efficient extension for distributed environments in which raw data or large spline design matrices cannot be transferred. Adequate aggregating these summaries capture the information of an surrogate likelihood of the VCMM and supports a one-step estimator that attains the same first-order efficiency as the centralized maximum-likelihood estimator. Further SVD-enhanced implementation ensures numerical stability under high-dimensional spline bases and strongly correlated random effects. Together, the centralized and communication-efficient methodologies provide a coherent and scalable toolkit for VCMM estimation—offering statistical optimality when communication is unrestricted and substantial computational and storage advantages when data must remain distributed.

The practical value of the proposed framework is further demonstrated through a large-scale analysis of U.S. internal migration linked to federally declared disasters—representing, to our knowledge, the first study to fit a full VCMM with millions of origin–destination flows while respecting communication constraints. Applying the methodology to commuting-zone–level data, the model uncovers rich spatial heterogeneity through its estimated push and pull effects, revealing a coherent geography of migration attractivity and repulsiveness across the United States. The time-varying coefficients further capture long-run macroeconomic cycles and disaster-related dynamics, yielding interpretable temporal responses that align with major economic shifts, reconstruction periods, and changes in regional resilience. Together, these findings illustrate that communication-aware, sufficient-statistics–based VCMM esti-

mation can deliver production-level throughput on massive spatiotemporal systems while preserving main statistical efficiency and principled uncertainty quantification.

Future research may extend the VCMM framework into an adaptive, real-time inference system capable of instant model updating and decision support. A streaming version of the sufficient-statistics estimator would allow parameters to be updated incrementally as new data arrive, using previously stored Fisher information to perform efficient one-step corrections without reprocessing historical records. Embedding these online updates into state-space or control formulations would enable the model to react dynamically to evolving spatiotemporal signals, while decision-theoretic modules translate predictive uncertainty into actionable recommendations. A complementary direction is to integrate VCMMs with mechanistic migration simulators—such as agent-based or gravity-type models—which provide generative structure for demographic flows and hazard-driven displacement. Combining these simulators with communication-aware statistical inference, following recent advances in optimal simulator selection and data-simulation fusion (Hung et al., 2023), would enable fast, scalable, and scientifically grounded forecasting for large-scale problems in climate adaptation, disaster response, and population redistribution.

References

Cai, D., Chen, X., and He, X. (2015). Robust and efficient large-scale matrix decomposition using randomized techniques. *IEEE Transactions on Knowledge and Data Engineering*, 27:1947–1959.

Cai, X., Xue, L., Pu, X., and Yan, X. (2021). Efficient estimation for varying-coefficient mixed effects models with functional response data. *Metrika*, 84:467–495.

Chen, H. and Wang, Y. (2011). A penalized spline approach to functional mixed effects model analysis. *Biometrics*, 67:861–870.

Chen, T., Habans, R., Douthat, T., Losh, J., Dehkharghani, L. C. J., and Lin, L.-H. (2025). Exact inference for transformed large-scale varying coefficient models with applications. *Journal of Data Science*, 23:353–369.

Chen, X. and Xie, M.-G. (2014). A split-and-conquer approach for analysis of extraordinarily large data. *Statistica Sinica*, 24:1655–1684.

De Boor, C. (1978). *A Practical Guide to Splines*. Springer, New York.

Drineas, P., Magdon-Ismail, M., Mahoney, M. W., and Woodruff, D. P. (2012). Fast approximation of matrix coherence and statistical leverage. *The Journal of Machine Learning Research*, 13:3475–3506.

Dunson, D. B. et al. (2008). *Random effect and latent variable model selection*. Springer.

Eilers, P. H. C. and Marx, B. D. (1996). Flexible smoothing with B-splines and penalties. *Statistical Science*, 11:89–121.

Fan, J., Guo, Y., and Wang, K. (2023). Communication-efficient accurate statistical estimation. *Journal of the American Statistical Association*, 118:1000–1010.

Fields, G. S. (1979). Place-to-place migration: Some new evidence. *The Review of Economics and Statistics*, pages 21–32.

Franco-Villoria, M., Ventrucci, M., and Rue, H. (2019). A unified view on bayesian varying coefficient models. *Electronic Journal of Statistics*, 13:5334–5359.

Guhaniyogi, R., Li, C., Savitsky, T. D., and Srivastava, S. (2022). Distributed bayesian varying coefficient modeling using a gaussian process prior. *Journal of Machine Learning Research*, 23:1–59.

Gurak, D. T. and Caces, F. (1992). Migration networks and the shaping of migration systems. *International migration systems: A global approach*, 150:176.

Habans, R. and Douthat, T. (2024). *Past and future migration in coastal Louisiana*. Open ICPSR, Ann Arbor, MI. <https://doi.org/10.3886/E210228V2>.

Halko, N., Martinsson, P.-G., and Tropp, J. A. (2011). Finding structure with randomness: Probabilistic algorithms for constructing approximate matrix decompositions. *SIAM Review*, 53:217–288.

Harville, D. A. (1977). Maximum likelihood approaches to variance component estimation and related problems. *Journal of the American Statistical Association*, 72:320–340.

Hastie, T. and Tibshirani, R. (1993). Varying-coefficient models. *Journal of the Royal Statistical Society: Series B*, 55:757–779.

Hoover, D. R., Rice, J. A., Wu, C. O., and Yang, L.-P. (1998). Nonparametric smoothing estimates of time-varying coefficient models with longitudinal data. *Biometrika*, 85:809–822.

Huang, C. and Huo, X. (2019). A distributed one-step estimator. *Mathematical Programming*, 174:41–76.

Hung, Y., Lin, L.-H., and Wu, C. J. (2022). Varying coefficient frailty models with applications in single molecular experiments. *Biometrics*, 78(2):474–486.

Hung, Y., Lin, L.-H., and Wu, C. J. (2023). Optimal simulator selection. *Journal of the American Statistical Association*, 118:1264–1271.

Jordan, M. I., Lee, J. D., and Yang, Y. (2019). Communication-efficient distributed statistical inference. *Journal of the American Statistical Association*, 114:668–681.

Lee, J. D., Liu, Q., Sun, Y., and Taylor, J. E. (2017). Communication-efficient sparse regression. *Journal of Machine Learning Research*, 18:1–30.

Li, L. and Wang, L. (2010). Varying coefficient models with longitudinal data: A spline-based approach. *Journal of Multivariate Analysis*, 101:372–386.

Li, M., Andersen, D. G., Park, J. W., Smola, A. J., Ahmed, A., Josifovski, V., Su, J., and Long, E. Y. (2014). Scaling distributed machine learning with the parameter server. In *Proceedings of the 11th USENIX Symposium on Operating Systems Design and Implementation*, pages 583–598.

Li, Y., Nguyen, D. V., Kürüm, E., Rhee, C. M., Chen, Y., Kalantar-Zadeh, K., and Şentürk, D. (2020). A multilevel mixed effects varying coefficient model with multilevel predictors and random effects for modeling hospitalization risk in patients on dialysis. *Biometrics*, 76:924–938.

Liberty, E., Woolfe, F., Martinsson, P.-G., Rokhlin, V., and Tygert, M. (2007). Randomized algorithms for the low-rank approximation of matrices. *Proceedings of the National Academy of Sciences*, 104:20167–20172.

Lindstrom, M. J. and Bates, D. M. (1988). Newton—Raphson and em algorithms for linear mixed-effects models for repeated-measures data. *Journal of the American Statistical Association*, 83:1014–1022.

Lu, Y. and Zhang, R. (2009). Smoothing spline estimation of generalized varying-coefficient mixed model. *Journal of Nonparametric Statistics*, 21:815–825.

Luo, C., Islam, M. N., Sheils, N. E., Buresh, J., Reps, J., Schuemie, M. J., Ryan, P. B., Edmondson, M., Duan, R., Tong, J., et al. (2022). DLMM as a lossless one-shot algorithm for collaborative multi-site distributed linear mixed models. *Nature Communications*, 13:1678.

McCulloch, C. E. and Searle, S. R. (2004). *Generalized, linear, and mixed models*. John Wiley & Sons.

McMichael, C., Barnett, J., and McMichael, A. J. (2012). An ill wind? Climate change, migration, and health. *Environmental health perspectives*, 120:646–654.

Meng, X., Saunders, M. A., and Mahoney, M. W. (2014). LSRN: A parallel iterative solver for strongly over- or underdetermined systems. *SIAM Journal on Scientific Computing*, 36:C95–C118.

Moore, C. M., MaWhinney, S., Carlson, N. E., and Kreidler, S. (2020). A bayesian natural cubic B-spline varying coefficient method for non-ignorable dropout. *BMC Medical Research Methodology*, 20:250.

Morris, J. S. and Carroll, R. J. (2006). Wavelet-based functional mixed models. *Journal of the Royal Statistical Society Series B: Statistical Methodology*, 68:179–199.

Paglino, E. (2024). Estimating excess migration associated with tropical storms in the USA 1990–2010. *Population and Environment*, 46:11.

Patterson, H. D. and Thompson, R. (1971). Recovery of inter-block information when block sizes are unequal. *Biometrika*, 58:545–554.

Porojan, A. (2001). Trade flows and spatial effects: the gravity model revisited. *Open Economies Review*, 12:265–280.

Qiu, Y., Mei, J., Guennebaud, G., and Niesen, J. (2024). RSpectra: Solvers for large-scale eigenvalue and svd problems (r package version 0.16-2). <https://CRAN.R-project.org/package=RSpectra>. Published 2024-07-18.

Rao, C. R. (1971). Minimum variance quadratic unbiased estimation of variance components. *Journal of Multivariate Analysis*, 1:445–456.

Ruppert, D., Wand, M. P., and Carroll, R. J. (2003). *Semiparametric Regression*. Number 12. Cambridge University Press.

Searle, S. R., Casella, G., and McCulloch, C. E. (2009). *Variance Components*. John Wiley & Sons.

Silverman, B. W. (1985). Some aspects of the spline smoothing approach to non-parametric regression curve fitting. *Journal of the Royal Statistical Society: Series B (Methodological)*, 47:1–21.

Tutz, G. and Kauermann, G. (2003). Generalized linear random effects models with varying coefficients. *Computational Statistics & Data Analysis*, 43:13–28.

Wahba, G. (1978). Improper priors, spline smoothing and the problem of guarding against model errors in regression. *Journal of the Royal Statistical Society Series B: Statistical Methodology*, 40:364–372.

Wang, J., Kolar, M., Srebro, N., and Zhang, T. (2017). Efficient distributed learning with sparsity. In *International Conference on Machine Learning*, pages 3636–3645. PMLR.

Wang, L. and Huang, J. Z. (2008). Random effect varying-coefficient models for longitudinal data. *Journal of Multivariate Analysis*, 99:129–151.

Wood, S. N. (2017). *Generalized Additive Models: An Introduction with R*. CRC Press, 2 edition.

Zhang, D. and Lin, X. (2004). Variance component testing in generalized linear mixed models. *Biometrika*, 91:133–148.

Zhang, Y., Duchi, J. C., and Wainwright, M. J. (2015). Divide and conquer kernel ridge regression. *Conference on Learning Theory*, pages 592–617.

Zhang, Y. and Shen, D. (2015). Estimation of semi-parametric varying-coefficient spatial panel data models with random-effects. *Journal of Statistical Planning and Inference*, 159:64–80.